# THE STRUCTURE OF PUCHERITE, $BiVO_4$

M. M. Qurashi[1] and W. H. Barnes, *Division of Physics, National Research Council, Ottawa, Canada.*

Abstract

The structure of pucherite, $BiVO_4$, ($a=5.33_2$A, $b=5.06_0$A, $c=12.02_0$A, $Z=4$, space group *Pnca*) has been analysed by Patterson projections and refined by Fourier and ($F_o-F_c$) syntheses. Atomic coordinates and interatomic distances are given. A preliminary structure reported earlier has been confirmed except for the positions of eight O in two sets of special positions that are now shown to be in general positions. An interesting relationship between the BiOCl structure and those of $BiVO_4$ and tetragonal $BiAsO_4$ is demonstrated.

## Introduction

In any general study of the role of vanadium in the structures of the vanadium minerals (Barnes & Qurashi, 1952), mixed oxides form a logical bridge between the oxides of vanadium, such as $V_2O_5$ (Ketelaar, 1936; Byström, Wilhelmi & Brotzen, 1950), and the more complex vanadates. It is, therefore, of interest to obtain reasonably accurate interatomic distances in a structure such as that of pucherite, $BiVO_4$. A preliminary structure for this mineral has been proposed (Quarashi & Barnes, 1952). In the present paper details of the analysis of Patterson projections are given and the refinement of the structure by Fourier and difference syntheses is described.

## Intensity Data

The intensity data for the three principal zones were collected by means of Buerger precession photographs using Mo $K_\alpha$ radiation ($\lambda=0.7107$A) and $\bar{\mu}=25°$. The crystal fragments were almost cubical in shape with linear dimensions of the order of 50 to 80 microns. Even for crystals as small as these, absorption corrections are significant; they were determined by standard graphical methods. Intensities were estimated visually from series of graded exposures (i.e., multiple exposures, not multiple *film* exposures as stated previously), using internal standards of intensity, since multiple film technique is not applicable to precession photographs. A later estimation of the intensities showed a standard deviation of about 15% compared with the earlier one. Taking this figure as a measure of the probable accuracy of the observations, the structure factors obtained from them should be accurate to about 8%. Lorentz-polarization factors were determined graphically with the aid of formulae given by Evans, Tilden & Adams (1949) and by Waser (1951). The observed intensities were placed on an absolute scale by the method

[1] National Research Laboratories Postdoctorate Fellow.

of Wilson (1942; also, see Harker, 1948), wherein a graph of log $(\sum_j f_j^2/\bar{I}_{obs.})$ is plotted against $(\sin\theta/\lambda)^2$ and the scale factor is obtained by finding the intercept at $(\sin\theta/\lambda)^2=0$. This procedure gives correct scaling to within about 10%.

## Patterson Projections

Patterson projections for the *h*0*l* and 0*kl* zones are shown in Fig. 1. For these syntheses the intensities were scaled only approximately, and the scale for the 0*kl* projection is about 20% lower than that for the *h*0*l*. A converging factor of $\exp(-4(\sin\theta/\lambda)^2)$ was applied because the observed intensities are appreciable even for reflections of the highest indices. From the fact that the height of a Patterson peak is approximately proportional to the product of the scattering factors of the two atoms giving rise to the peak, the peak heights for the various vectors can be deduced. Thus, taking the average height of the origin peaks (135 and 110) of the two projections (Fig. 1) as 122, the following estimates of the

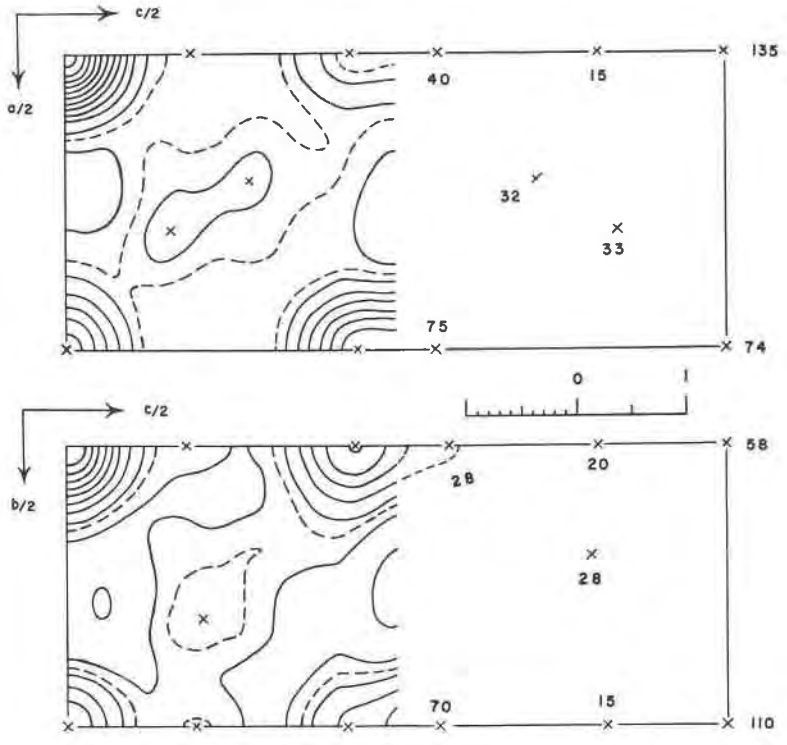


Fig. 1. Patterson projections of pucherite (scale in A).

peak heights of unit weight are obtained: Bi-Bi, 28; Bi-V, 7.0; Bi-O, 2.8; V-V, 1.7; V-O, 0.6; O-O, 0.2. It is clear that peaks due to V-V, V-O, and O-O will have almost negligible heights compared with the others and are unlikely to show up clearly on the Patterson maps. Analysis of the Patterson projections, therefore, must be confined largely to the identification of the peaks due to Bi-Bi, Bi-V, and Bi-O.

Retaining the same orientation for pucherite as selected previously (Qurashi & Barnes, 1952) to conform to the axial lengths of de Jong and de Lange (1936), $b<a<c$, the coordinates of the equivalent positions in the (centro-symmetrical) space group *Pnca* ($D_{2h}^{14}$) are

(*a*) $000;\ \frac{1}{2}00;\ 0\frac{1}{2}\frac{1}{2};\ \frac{1}{2}\frac{1}{2}\frac{1}{2}$,

(*b*) $00\frac{1}{2};\ \frac{1}{2}0\frac{1}{2};\ 0\frac{1}{2}0;\ \frac{1}{2}\frac{1}{2}0$,

(*c*) $\frac{1}{4}0z;\ \frac{3}{4}0\bar{z};\ \frac{1}{4}\frac{1}{2},\ \frac{1}{2}+z;\ \frac{3}{4}\frac{1}{2},\ \frac{1}{2}-z$,

(*d*) $xyz;\ \frac{1}{2}+x,\ \frac{1}{2}-y,\ \frac{1}{2}-z;\ \bar{x},\ \frac{1}{2}+y,\ \frac{1}{2}-z;\ \frac{1}{2}-x,\ \bar{y},\ z$;
and these with changed signs.

Since there are only 4 Bi per unit cell, they must occupy one of the sets of special positions (*a*), (*b*), or (*c*). Now there are peaks in the Patterson maps (Fig. 1) at $(\frac{1}{2},\ -,\ 0)$ and $(-,\ \frac{1}{2},\ 0)$ with observed heights of 74 and 58, respectively. It is unlikely, however, that these arise from Bi atoms in positions (*a*) or (*b*) because such sites for Bi would result in a Patterson peak height of $4\times28=112$, or more. (It will be shown later that they are, in fact, due largely to Bi-V vectors). The Bi atoms, therefore, must be in positions (*c*). This deduction is supported by the presence of Patterson peaks (Fig. 1) at $(\frac{1}{2},\ -,\ \frac{1}{6}\frac{3}{0})$ and $(-,\ 0,\ \frac{1}{6}\frac{3}{0})$ which are the highest (75 and 70) observed. Thus a typical Bi-Bi peak is located at $(\frac{1}{2},\ 0,\ \frac{1}{6}\frac{3}{0})$. The coordinates of the Bi atoms, in special positions (*c*), therefore, are established as $(\frac{1}{4},\ 0,\ 0.108)$, etc., and the calculated height of a corresponding Bi-Bi Patterson peak is $2\times28=56$.

Since the 4V also must be in positions (*a*), (*b*), or (*c*), Bi-V Patterson peaks must occur with $x$ equal to 0, $\frac{1}{4}$, or $\frac{1}{2}$, and $y$ equal to 0 or $\frac{1}{2}$. Therefore, the peaks previously examined at $(\frac{1}{2},\ -,\ 0)$ and $(-,\ \frac{1}{2},\ 0)$, of observed heights 74 and 58, together with those at $(0,\ -,\ \frac{1}{6}\frac{3}{0})$ and $(-,\ \frac{1}{2},\ \frac{1}{6}\frac{3}{0})$, of observed heights 40 and 28 (see Fig. 1), can be identified as Bi-V. They constitute a set of the second highest peaks in the two Patterson projections.

From the presence of two Bi-V peaks having $z=\frac{1}{6}\frac{3}{0}$ it follows that the V atoms must also be in special positions (*c*) but with coordinates $(\frac{1}{4},\ 0,\ \frac{1}{2}-\frac{1}{6}\frac{3}{0})$, etc. The calculated heights of corresponding Patterson peaks are $8\times7.0=56$ at $z=0$ and $4\times7.0=28$ at $z=\frac{1}{6}\frac{3}{0}$. It may now be noted that the calculated values for the Bi-Bi Patterson peaks should be increased by about 6% since the V-V and Bi-Bi vectors coincide.

Finally the remaining Patterson peaks in Fig. 1 presumably must be

Bi-O since the heights of those due to V-V, V-O, and O-O, would certainly be less than 10.

As may be appreciated, the precise location of the 16 oxygen atoms in the unit cell is more difficult. The presence of Patterson peaks at $x$, $y \sim \frac{1}{4} \pm \frac{1}{30}$ shows that at least eight must be in general positions ($d$) with approximate coordinates $(-\frac{1}{30}, \frac{1}{4}+\frac{1}{30}, \frac{1}{4}-\frac{1}{30})$, etc., as given previously (Qurashi & Barnes, 1952, p. 424). The remaining eight O were placed originally in special positions ($a$) and ($b$) on the basis of the small Patterson peaks (observed heights, approximately 15) along $x$, $y=0, \frac{1}{2}$. Refinement of the structure has shown that this deduction is incorrect. Some indication of possible misinterpretation of these small peaks is given by the calculated value of 15 (against the observed 30) for the Patterson peaks along $x$, $y \sim \frac{1}{4} \pm \frac{1}{30}$ (after making allowance for V-O interactions and overlapping) if only eight O are placed in general positions. This, however, is not very conclusive due to the "background" usually present in Patterson maps.

## Fourier Projections

The analysis of the Patterson projections fixes the positions of the bismuth and vanadium atoms with considerable certainty. Since the contribution of the oxygen atoms to the structure factor for any given reflection generally will be much less than that of the metal atoms, it should be possible to obtain the signs of most of the structure factors from the metal atom contributions alone.

The structure factor data are given in Table 1, where the values of F calculated for the metal atoms ($F_{c(m)}$) may be compared with the observed structure factors ($|F_0|$). In only one case, (017), is there any real doubt regarding the sign of any of the observed $h0l$ and $0kl$ reflections. (Fortunately $|F_0|$ for 017 is small so that it could be omitted from the preliminary Fourier synthesis without risk of serious error.) Using the signs so determined, the $ac$ and $bc$ Fourier projections were calculated, with a converging factor of $\exp(-3(\sin\theta/\lambda)^2)$, and are shown in Fig. 2. They are particularly interesting because all the oxygen atoms emerge quite clearly in two sets of eight-fold positions.

The observed Patterson peaks in Fig. 1, for which $x$, $y \sim \frac{1}{4}$, can now be assigned to Bi-O vectors, while those of height 15, along $x$, $y=0$ (Fig. 1), correspond to the small bulges in the Fourier maps (Fig. 2) near the bismuth atoms and probably are due to diffraction effects and cumulative observational errors.

While the Fourier projections of Fig. 2 show the four-fold coordination of oxygen atoms around the atoms of vanadium, they are consistent with two possible arrangements, one of which is nearly tetrahedral and the

TABLE 1. STRUCTURE FACTOR DATA FOR *h0l* AND *0kl* ZONES ($|F_0|$, OBSERVED; $F_{c(m)}$, CALCULATED FOR METAL ATOMS ONLY; $F_c$, CALCULATED WITH FINAL COORDINATES)

| *hkl* | $F_{c(m)}$ | $\|F_0\|$ | $F_c$ | *hkl* | $F_{c(m)}$ | $\|F_0\|$ | $F_c$ |
|---|---|---|---|---|---|---|---|
| 000 | 404 | 552 | 552 | 011 | 164 | 188 | 160 |
| 002 | 78 | 83 | 84 | 013 | $\overline{88}$ | 59 | $\overline{64}$ |
| 004 | $\overline{298}$ | 242 | $\overline{254}$ | 015 | $\overline{174}$ | 188 | $\overline{186}$ |
| 006 | $\overline{166}$ | 126 | $\overline{127}$ | 017 | 6 | 28 | 29 |
| 008 | 154 | 135 | 136 | 019 | 131 | 112 | 125 |
| 0.0.10 | 172 | 182 | 167 | 0.1.11 | 43 | <35 | 26 |
| 0.0.12 | $\overline{47}$ | 61 | $\overline{69}$ | 0.1.13 | $\overline{79}$ | 76 | $\overline{72}$ |
| 0.0.14 | $\overline{137}$ | ~190 | $\overline{131}$ | 020 | 308 | 314 | 251 |
| 102 | $\overline{202}$ | 190 | $\overline{190}$ | 022 | 63 | <50 | 35 |
| 104 | $\overline{79}$ | 41 | $\overline{56}$ | 024 | $\overline{249}$ | 305 | $\overline{273}$ |
| 106 | 136 | 145 | 161 | 026 | $\overline{145}$ | 142 | $\overline{149}$ |
| 108 | 110 | 90 | 96 | 028 | 137 | 147 | 140 |
| 1.0.10 | $\overline{59}$ | 66 | $\overline{77}$ | 0.2.10 | 156 | 146 | 140 |
| 1.0.12 | $\overline{99}$ | 81 | $\overline{79}$ | 0.2.12 | $\overline{44}$ | 39 | $\overline{40}$ |
| 200 | $\overline{313}$ | 285 | $\overline{234}$ | 031 | 123 | 113 | 118 |
| 202 | $\overline{65}$ | 51 | $\overline{60}$ | 033 | $\overline{68}$ | 81 | $\overline{98}$ |
| 204 | 252 | 290 | 273 | 035 | $\overline{136}$ | 96 | $\overline{114}$ |
| 206 | 147 | 145 | 153 | 037 | 5 | <35 | $\overline{2}$ |
| 208 | $\overline{139}$ | 169 | $\overline{162}$ | 039 | 108 | 91 | 105 |
| 2.0.10 | $\overline{157}$ | 145 | $\overline{135}$ | 0.3.11 | 37 | 24 | 31 |
| 2.0.12 | 44 | 40 | 39 | 040 | 207 | 207 | 198 |
| 302 | 158 | 192 | 173 | 042 | 43 | 59 | 66 |
| 304 | 63 | 44 | 51 | 044 | $\overline{176}$ | 155 | $\overline{159}$ |
| 306 | $\overline{110}$ | 86 | $\overline{91}$ | 046 | $\overline{104}$ | 80 | $\overline{92}$ |
| 308 | $\overline{91}$ | 53 | $\overline{60}$ | 048 | 103 | 100 | 110 |
| 3.0.10 | 51 | 63 | 72 | 0.4.10 | 123 | 100 | 98 |
| 3.0.12 | 88 | 80 | 80 | 051 | 85 | 72 | 83 |
| 400 | 215 | 228 | 227 | 053 | $\overline{46}$ | 38 | $\overline{38}$ |
| 402 | 44 | <35 | 33 | 055 | $\overline{95}$ | 69 | $\overline{81}$ |
| 404 | $\overline{181}$ | 170 | $\overline{170}$ | 057 | 3 | <35 | 10 |
| 406 | $\overline{110}$ | 92 | $\overline{89}$ | 060 | 135 | 130 | 122 |
| 408 | 108 | 94 | 96 | | | | |
| 4.0.10 | 127 | 123 | 114 | | | | |
| 502 | $\overline{107}$ | 80 | $\overline{89}$ | | | | |
| 504 | $\overline{44}$ | <35 | $\overline{31}$ | | | | |
| 506 | 79 | 80 | 98 | | | | |
| 508 | 69 | 52 | 58 | | | | |
| 600 | $\overline{144}$ | 136 | $\overline{129}$ | | | | |
| 602 | $\overline{30}$ | 34 | $\overline{33}$ | | | | |
| 604 | 125 | ~93 | 112 | | | | |

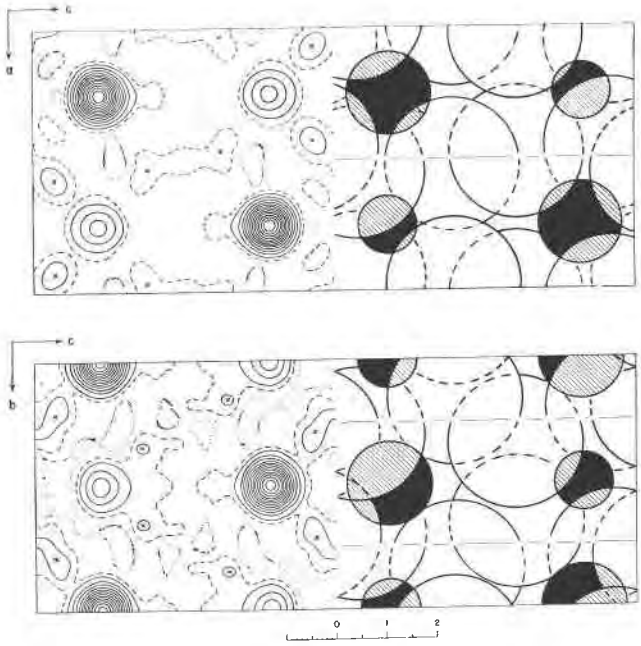


FIG. 2. Pucherite, $BiVO_4$, $h0l$ & $0kl$ projections (scale in A). Fourier maps on left; contours at intervals of $10e.A^{-2}$ with the $5e.A^{-2}$ line broken; zero contours dotted; approximate O positions indicated by crosses. Schematic structure on right; small solid circles, V; large solid circles, Bi; very large open circles, O; solid circles are hatched where overlaid by O.

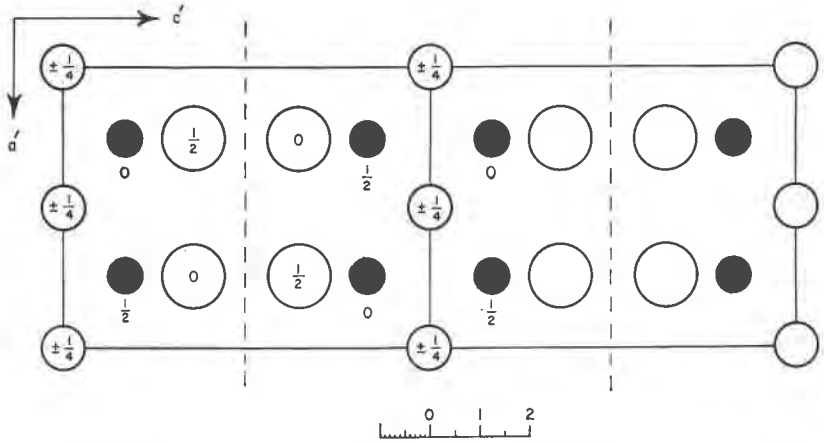


FIG. 3. Bi0Cl, $h'0l'$ projection (scale in A); solid circles, Bi; small open circles, O; large open circles, Cl.

other is nearly planar. Although the planar coordination can be rejected on spatial grounds and because it would require a shortest O-O distance of 2.06A, it is of interest to examine the $hk0$ zone for possible information. The zero level, $c$ axis, precession photograph, therefore, is reproduced in Fig. 4 and it will be seen that all reflections with both $h$ and $k$ even are equally strong when allowance is made for Lorentz-polarization and scattering factors. While this is in agreement with the proposed structure, for which $F_{hk0}=4f_{Bi}+4f_V+$(oxygen contributions), when $h$ and $k$ are both even, it is clearly not suitable for establishing the configuration of the oxygen atoms. Due to the $a$ glide, the only other observable reflections in this zone have $h$ even and $k$ odd. In Table 2, the estimated structure factors ($|F_0|$) for these few reflections are compared with those calculated for a planar arrangement of the oxygen atoms ($F_{c(p)}$) and for a tetrahedral arrangement ($F_{c(t)}$), respectively; agreement with $|F_0|$ is better for the tetrahedral coordination. It is obvious, from the small values of $F_0$ for these reflections, that the corresponding spots will not be visible in the reproduction (Fig. 4).

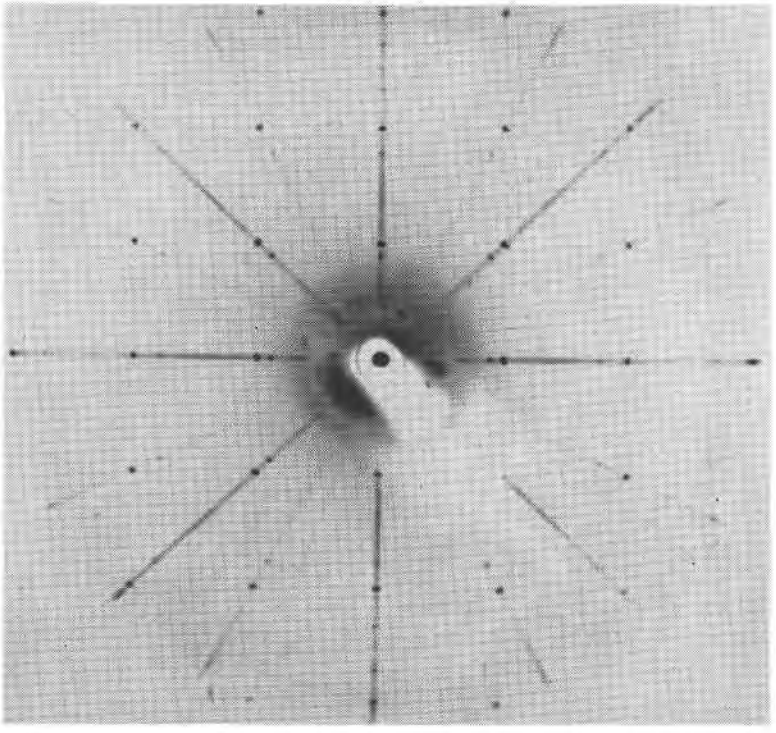

FIG. 4. Pucherite, $c$ axis zero-level precession photograph; $b^*$, horizontal; $a^*$, vertical; (unfiltered Mo radiation).

Although the salient features of the pucherite structure are brought out reasonably well by the Fourier projections of Fig. 2, the oxygen contours and peak heights are not entirely satisfactory. This is largely the result of diffraction (i.e., series termination) effects and can be overcome by means of successive difference syntheses.

TABLE 2. STRUCTURE FACTORS FOR *hk0* ZONE; *h* EVEN, *k* ODD ($|F_0|$, OBSERVED; $F_{c(p)}$, CALCULATED FOR PLANAR OXYGENS; $F_{c(t)}$, CALCULATED FOR TETRAHEDRAL OXYGENS)

| *hk*0 | $F_{c(p)}$ | $\|F_0\|$ | $F_{c(t)}$ |
|---|---|---|---|
| 210 | 34 | 10 | 13 |
| 230 | $\bar{1}0$ | 16 | $\bar{1}\bar{5}$ |
| 410 | 28 | <20 | 9 |
| 430 | $\bar{9}$ | <20 | $\bar{1}\bar{5}$ |

## REFINEMENT BY DIFFERENCE SYNTHESES

Structure factors for all observable reflections were calculated using atomic positions obtained from the Fourier maps of Fig. 2. Atomic scattering factors were obtained from the *Internationale Tabellen* (1935). Since the state of ionization of the atoms is uncertain, estimates were made for $Bi^{+1.5}$, $V^{+2.5}$, $O^{-1}$. A temperature factor, $\exp(-B(\sin\theta/\lambda)^2)$ was employed to simulate experimental conditions. During refinement, values of B, obtained by plotting $|F_c|/|F_0|$ as functions of $(\sin\theta/\lambda)^2$, altered from $-1.0$ to $-1.3A^2$. The final value corresponds to a thermal vibration of amplitude 0.13A. This is reasonable although much reliance cannot be placed on the absolute value of B.

Fourier syntheses were made using $(F_0-F_c)$ in place of $F_0$ and the

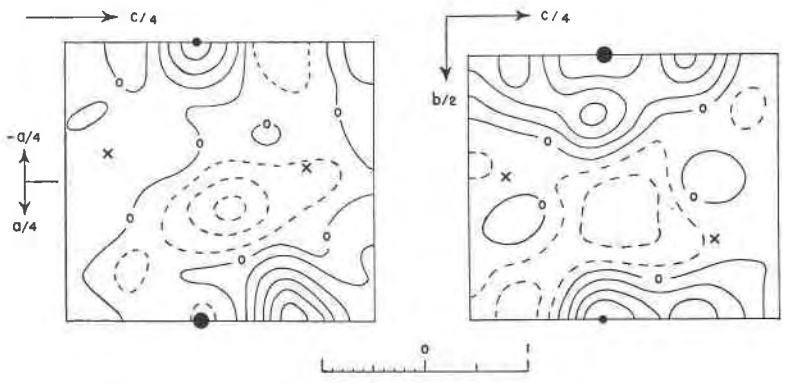


FIG. 5. Pucherite, $BiVO_4$, difference $(\rho_0-\rho_c)$ maps (scale in A); contours at intervals of $1e.A^{-2}$ with zero contour labelled and negative contours broken; small solid circles, V; larger solid circles, Bi; O positions indicated by crosses.

resulting difference projections were plotted. Cochran (1951) and others have described how shifts in atomic coordinates and other details are determined from such data. The final difference maps, obtained after three successive refinements, are shown in Fig. 5. The criterion for correctness of the coordinates used in the calculations is that the gradient should be zero at all atomic positions. This is fulfilled in the maps of Fig. 5, with the exception of one oxygen position in the *h*0*l* projection which requires a shift of −0.01A in the $x$ coordinate.

It will be observed that ripples are prominent in the neighbourhood of the metal atoms. The peaks surrounding the bismuth atoms cannot be interpreted as due to any appreciable excess thermal vibration, nor can the large positive peak at the vanadium position be taken as indicating a smaller value of B in the temperature factor because the necessary reduction would make B negative for vanadium. Since the peak at the vanadium position appears in both difference projections (Fig. 5) it may be genuine, and not simply the result of cumulative errors. In this case it may conceivably be due to the poor approximation of the Thomas-Fermi scattering curves for a light atom such as vanadium.

The final atomic coordinates are collected in Table 3 together with standard deviation, $\sigma(u)$, for each. The latter were obtained by calculating the root-mean square gradient $\sqrt{\overline{(\partial D/\partial u)^2}}$, and using the formula $\sigma(u)=\sqrt{\overline{(\partial D/\partial u)^2}}/2p\rho(0)$ (*cf.*, Cochran, 1951, pp. 83, 89), where $D=(\rho_0-\rho_c)$ is the electron density in the difference map. It will be noticed in Table 3 that the scatter of the $z$ coordinates about the mean values for the two projections is of the order of the corresponding estimated $\sigma(z)$ in the case of oxygen, but is considerably greater than $\sigma(z)$ in the case of

Table 3. Atomic Coordinates (in A) and Standard Deviations
($a=5.33_2$A, $b=5.06_0$A, $c=12.02_0$A)

| | $x$ | $y$ | $z$ | $z$ (mean) | $\sigma(x)$ | $\sigma(y)$ | $\sigma(z)$ |
|---|---|---|---|---|---|---|---|
| Bi | 5.332/4 | — | 1.325 | | | | |
| | | | | 1.318 | 0 | 0 | 0.003 |
| | — | 0 | 1.311 | | | | |
| V | 5.332/4 | — | 4.754 | | | | |
| | | | | 4.734 | 0 | 0 | 0.011 |
| | — | 0 | 4.715 | | | | |
| $O_I$ | −0.28 | — | 0.42 | | | | |
| | | | | 0.38 | 0.04 | 0.05 | 0.03 |
| | — | −1.16 | 0.34 | | | | |
| $O_{II}$ | −0.16 | — | 2.32 | | | | |
| | | | | 2.35 | 0.04 | 0.05 | 0.03 |
| | — | 1.77 | 2.38 | | | | |

the metal atoms. This is due in part to the fact that the $(F_0 - F_c)$ terms used in the final synthesis were weighted inversely as the probable errors in the estimations of $|F_0|$. This procedure gives the weaker reflections proportionately greater weight, and ultimately improves the accuracy of the oxygen parameters.

The standard deviations are lowest for the $z$ coordinates because the final values were averaged over both projections.

Values of $F_c$, calculated with the coordinates of Table 3, will be found in Table 1. The reliability index, $R = \sum[|F_0| - |F_c|]/\sum|F_c|$, is 0.10 for each zone. This compares favourably with the estimated error in $F_0$ of about 8%.

## Interatomic Distances, and Discussion

The bonding of both kinds of metal atoms to their nearest oxygen atoms shows clearly in the Fourier maps (Fig. 2), but, whereas V atoms are bonded only to four O atoms, the Bi atoms have additional bonds to O atoms across $z=0$ and $z=\frac{1}{4}$. The interatomic distances are given in Table 4.

Table 4. Interatomic Distances (in A)

| | | |
|---|---|---|
| V-$O_I$, 1.95±0.07 | Bi-$O_I$, 2.20±0.06 | $O_I$-$O_I$, 2.50, 2.78; 3.14, 3.45 |
| V-$O_{II}$, 1.76±0.07 | Bi-$O_{II}$, 2.54±0.07 | $O_{II}$-$O_{II}$, 2.86, 2.97; 2.80, 3.33 |
| (V-$O_I'$, 2.69±0.07[1]) | Bi-$O_I'$, 2.31±0.06[1] | $O_I$-$O_{II}$, 3.04, 3.53; 2.80, 3.44 |
| (V-$O_{II}'$, 4.33±0.07[2]) | Bi-$O_{II}'$, 2.73±0.06[2] | |

[1] Across $z=0, \frac{1}{2}$.

[2] Across $z=\pm\frac{1}{4}$; standard error of O-O distances, 0.1A.

It is of interest to note that the $O_{II}$ atoms are bonded rather loosely to Bi but firmly to V, whereas the opposite is true of the $O_I$ atoms. In fact, the Bi-$O_{II}'$ distance (across $z=\pm\frac{1}{4}$) is so great (2.73A) as to suggest that most of the force across these planes must be due to O-O van der Waals interactions. This is apparent in the schematic structure comprising the right-hand side of Fig. 2, where radii approximately proportional to the ionic radii have been used for the circles representing the atoms.

The ratios of the univalent radii of the metal and oxygen atoms suggests six-fold coordination around vanadium. It is of interest to note that whereas such coordination occurs in tetragonal $V_2O_4$ (Wyckoff, 1948), it becomes intermediate between six-fold and four-fold in $V_2O_5$ (Ketelaar, 1936; Byström, Wilhelmi & Brotzen, 1950) and is clearly four-fold (tetrahedral) in pucherite, $BiVO_4$.

The univalent radius ratio favours either six-fold or eight-fold oxygen coordination around bismuth, depending on whether $Bi^{+5}$ or $Bi^{+3}$ is

involved. If the long (2.73A) Bi-$O_{II}'$ bonds are included, the pucherite structure shows eight-fold coordination with two pairs of short bonds (2.20A, 2.31A) and two pairs of long bonds (2.54A, 2.73A). This arrangement is analogous to that in BiOCl, which has the PbFCl layer type structure, with $a=3.883$A, $c=7.348$A, space group $P4/nmm$ (Wyckoff, 1948), and from which the structure of tetragonal $BiAsO_4$ (Mooney, 1948) and that of pucherite ($BiVO_4$) can be derived.

For direct comparison with the structure of pucherite, that of BiOCl is shown in projection in Fig. 3., where the diagonals of the unit cell of BiOCl have been taken as axes $a'=b'=5.49$A, and double the $c$ axis as $c'=14.70$A. By replacing one-half the number of Bi atoms with As and all the Cl atoms with O, the structure of tetragonal $BiAsO_4$ can be obtained by small displacements of the O positions and by slightly larger displacements of the Cl positions (compare Fig. 3 with Fig. 1*b* of previous paper, Qurashi & Barnes, 1952, p. 425). In order to obtain the $BiVO_4$ structure, after substitution of one-half the number of Bi atoms with V and all the Cl atoms with O, a shift of alternate layers (separated by the broken lines in Fig. 3) through $b'/2$, parallel to the $b'$ axis, is required.

The replacement of all the Cl atoms with O and of one-half the number of Bi atoms with V (or As) reduces the lengths of $a'$, $b'$, and especially $c'$, observed in BiOCl. The decrease in the short Bi-O separation from 2.31A in BiOCl to an average of $2.26\pm0.04$A (for Bi-$O_I$ and Bi-$O_{II}$) in $BiVO_4$ may be significant. In addition, the average V-O separation in $BiVO_4$ is $1.86\pm0.04$A (for V-$O_I$ and V-$O_{II}$) which is about 0.10A greater than the normal V-O distance for tetrahedrally coordinated $V^{+5}$ (*cf.* Ketelaar, 1936; Zachariasen, 1931). The oxygen coordination in pucherite, therefore, appears to be a compromise between configurations previously found for $Bi^{+3}$ in BiOCl and for $V^{+5}$ in $V_2O_5$. This suggests that the effective valence of Bi in $BiVO_4$ is somewhat greater than $+3$ while that of V is somewhat less than $+5$.

In BiOCl the predominant force holding the layers together across the planes $z=\pm\frac{1}{4}$ (see Fig. 3) is due to the Cl-Cl interactions since the Cl-Cl distance (3.48A) is much smaller than the radius sum while the Bi-Cl distance (3.49A) is significantly greater than the radius sum. It has already been pointed out that similar O-O interactions, rather than Bi-O forces, must be operative across the corresponding planes in pucherite (see Fig. 2). They are probably responsible for the perfect {001} cleavage.

In view of the interesting features of the pucherite structure, particularly the oxygen coordination around the metal ions, an attempt is being made to improve the accuracy of the metal-oxygen distances by a

three-dimensional analysis using difference syntheses. It is hoped to report more accurate coordinates and interatomic distances in a subsequent note.

Grateful acknowledgement is made to Professor Clifford Frondel for the specimen of pucherite (Harvard Museum, 101703) from Schneeberg, the type locality.

## References

Barnes, W. H. & Qurashi, M. M. (1952): Unit cell and space group data for certain vanadium minerals. *Am. Mineral.*, **37,** 407–422.

Byström, A., Wilhelmi, K. A. & Brotzen, O. (1950): Vanadium pentoxide—a compound with five-coordinated vanadium atoms, *Acta Chem. Scand.*, **4,** 1119–1130.

Cochran, W. (1951): The structures of pyrimidines and purines. *V.* The electron distribution in adenine hydrochloride, *Acta Cryst.*, **4,** 81–92.

de Jong, W. F. & de Lange, J. J. (1936): *X*-ray study of pucherite. *Am. Mineral.*, **21,** 809.

Evans, H. T., Tilden, S. G. & Adams, D. P. (1949): New techniques applied to the Buerger precession camera for *x*-ray diffraction studies. *Rev. Sci. Instr.*, **20,** 155–159.

Harker, D. (1948): Absolute intensity scale for crystal diffraction data. *Am. Mineral.*, **33,** 764–765.

*Internationale Tabellen zur Bestimmung von Kristallstrukturen* (1935), Berlin.

Ketelaar, J. A. A. (1936): Die Kristallstruktur des Vanadinpentoxyds. *Zeit. Krist.*, (A) **95,** 9–27.

Mooney, R. C. L. (1948): Crystal structure of tetragonal bismuth arsenate, $BiAsO_4$, *Acta Cryst.*, **1,** 163–165.

Qurashi, M. M. & Barnes, W. H. (1952): A preliminary structure for pucherite, $BiVO_4$, *Am. Mineral.*, **37,** 423–426.

Waser, J. (1951): The Lorentz factor for the Buerger precession method. *Rev. Sci. Instr.*, **22,** 563–566.

Wilson, A. J. C. (1942): Determination of absolute from relative *X*-ray intensity data, *Nature*, **150,** 152.

Wyckoff, R. W. G. (1948): *Crystal Structures*, vol. 1, chap. 4, New York.

Zachariasen, W. H. (1931): A set of empirical crystal radii for ions with inert gas configuration. *Zeit. Krist.*, (A) **80,** 137–153.